INTERNATIONAL JOURNAL FOR NUMERICAL AND ANALYTICAL METHODS IN GEOMECHANICS, VOL. 21, 295–311 (1997)

A DISCRETE ELEMENT STUDY OF THE RELATIONSHIP OF FABRIC TO WAVE PROPAGATIONAL BEHAVIOURS IN GRANULAR MATERIALS

QIMING TAI AND MARTIN H. SADD*

Department of Mechanical Engineering & Applied Mechanics, University of Rhode Island, Kingston, RI 02881, U.S.A.

SUMMARY

Wave propagation in granular materials is numerically studied through discrete element simulation. Two-dimensional (2-D) model material systems composed of large numbers of circular particles were numerically generated. The particles in these model materials were randomly distributed with a biasing algorithm to produce fabric anisotropy so as to create preferred directions within the material. Wave motion is introduced through dynamic loadings to appropriate boundary particles to produce horizontal and vertical plane wave propagation within each model material. Discrete element simulation with a non-linear hysteretic interparticle contact law is used to model the dynamic behaviour of the model granular systems, and this yields information on the wave speed and amplitude attenuation. Through the investigation of several model systems, relationships are established between wave propagational characteristics and granular microstructure or fabric. Specific fabric measures which were used included branch vectors, path microstructures and void characteristics. Distributions of these fabric descriptors were determined, and comparisons and correlations were made with the discrete element wave propagation results. Conclusions of this study indicated that while all three fabric measures provided some degree of correlation with the wave motion behaviours, the void fabric descriptor produced the best correlation for the assemblies under investigation. © 1997 by John Wiley & Sons, Ltd.

Int. J. Numer. Anal. Meth. Geomech., Vol. 21, 295–311 (1997)
(No. of Figures: 11 No. of Tables: 1 No. of Refs: 33)

Key words: wave propagation; discrete element modelling; granular materials; fabric; anisotropy; microstructure

INTRODUCTION

Granular materials are commonly described as a collection of distinct particles which can displace from one another with some degree of independence and which interact basically through contact mechanisms. The discrete nature of such materials establishes non-continuous and discrete load transfer behaviour which can be related to the material microstructure or fabric. For example, it has been well established[1–3] that load transfer in a dry cohesionless granular medium occurs along a complex network of discrete paths. With regard to wave propagation, granular materials create a structured wave-guide network through which mechanical energy is transferred. Along a given wave path, the dynamic load transfer is determined by the contact

*Correspondence to M. H. Sadd.

Contract grant sponsor: Air Force Office Scientific Research—Particulate Mechanics Program; contract grant number: F49620-89-C-0091; contract grant number: F49620-93-1-0209

CCC 0363–9061/97/050295–17$17.50

Received 10 August 1995
Revised 20 August 1996

interactions between neighbouring particles. The propagational characteristics of wave speed, amplitude attenuation and wave form dispersion are thus related to the local fabric and established wave paths.

Interest in dynamic geomechanics problems has produced considerable research over the past several decades, and numerous articles have appeared dealing with wave propagation in sand and rock materials. More recently over the past decade or two, research on granular material behaviour has focussed on using micromechanical modelling incorporating local mechanics at the particulate level to predict the macro-constitutive response. A considerable amount of work[4–14] has been done in modelling granular media as arrays of idealized (circular or spherical) elastic particles with the goal of determining equivalent macro elastic constitutive moduli from the local interparticle contact behaviour. Another large body of research dealing with microstructural effects in particulate media has used the approach of developing *fabric tensor theories*. Fabric of granular materials is normally described as the spatial arrangement of the solid particles and associated voids. Pioneering work by Oda *et al.*[15] and Nemat-Nasser and Mehrabadi,[16] and later followed by many other studies, e.g. References 17–19 have developed several types of tensorial quantities which characterize local microstructure (fabric) and which can be used to construct constitutive laws to predict observed behaviours. Although some success in linking fabric to mechanical behaviour has been obtained, no unique choice of fabric description has been universally accepted which can adequately describe the general mechanical response of particulate media.

Some research has categorized fabric into two types: *orientation fabric* (orientation of individual particles) and *packing fabric* (mutual relation of individual particles). Orientation fabric may be quantitatively defined by a vector mean direction and a vector magnitude to characterize orientation of non-spherical or non-circular particles. This fabric measure is commonly represented by an angular measure (with respect to a reference direction) of the long axes of individual

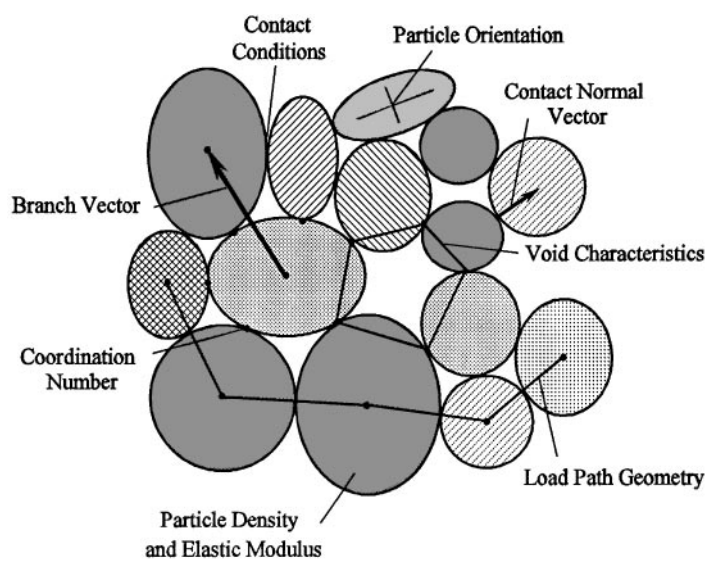

Figure 1. Typical microstructure or fabric in granular materials

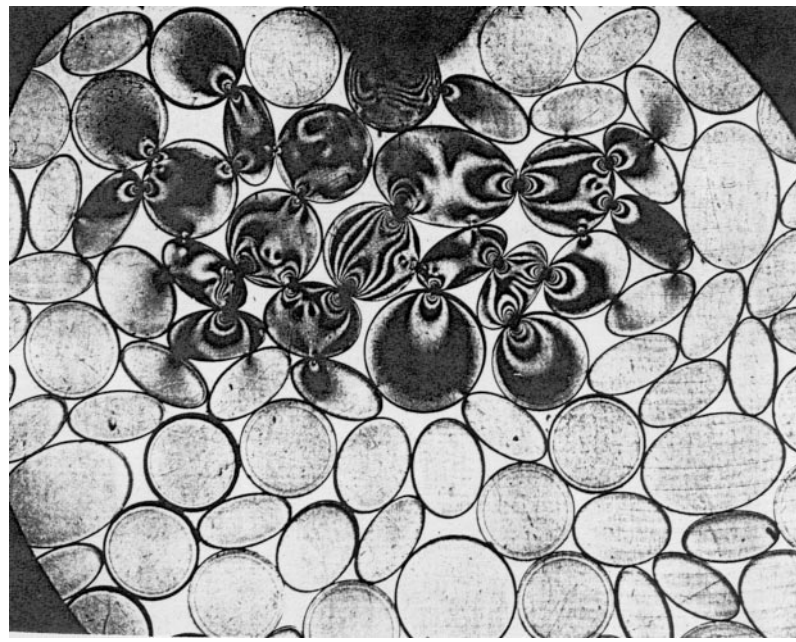

Figure 2. Dynamic photoelastic photograph of wave propagation in a model granular medium

particles. Packing fabric measures have included *branch vectors*, *normal contact vectors*, *co-ordination or contact numbers*, *void characteristics*, *etc*. Examples of these fabric measures are illustrated schematically in Figure 1. Some of these fabric measures are solely *kinematical* in nature, determined primarily by the particle shape and packing geometry. Other measures such as those related to the contact conditions are *kinetic*, and are determined by the particle material and shape properties and also by the contact surface conditions.

Figure 2 shows a high-speed photograph of the dynamic photoelastic fringe patterns associated with an actual wave moving (from top to bottom) through a model particulate medium containing some of these fabric structures. Using such experimental techniques, it has been observed[1–3] for both static and dynamic loading conditions that particulate materials transmit mechanical loadings along a series of complex discrete paths. These discrete paths are established, in relation to the loading direction, by many of the microstructural variables mentioned, and therefore local wave propagation is determined by granular fabric through the creation of local wave guides.

The article presents the results of a theoretical/numerical study which examines the relationship of granular fabric with wave propagational variables. The model granular materials under study were large random assemblies of circular particles created numerically using random media generator codes. Although these assemblies involved random assembly procedures, deliberate biasing was used in the generation process in order to construct materials with a variety of microstructures. Wave propagation through these model assemblies was simulated using the computational scheme of *discrete element modelling*. This study focusses primarily on the effects of packing fabric as measured by: *branch vector distributions* (which for circular particles coincide with normal contact vectors), *path fabric*, and *void polygon fabric*.

The modelling scheme presented here can be thought of as a *meso-domain* approach, attempting to bridge the micro–macro responses. Micromechanical modelling at the particulate level is applied to a sufficiently large assembly of particles such that averages of particular wave propagational characteristics will be meaningful. This issue is related to the *homogenization process* as discussed by Bourbié *et al.*[20] in which they point out that macroscopically meaningful results can only be found if the sample size is much larger than the minimum homogenization volume.

DISCRETE ELEMENT METHOD

Originally developed by Cundall and Strack,[21] the *discrete element method* is a numerical scheme that has been successfully used to simulate the response of granular media by modelling the dynamic behaviour of large assemblies of circular disks, spheres, and blocks.[22–28] The method makes simplifying constitutive assumptions for each particle (commonly assuming rigid body behaviour) and then uses Newtonian mechanics to determine the translational and rotational motion of each particle in the assembly. In order to establish interparticle contact behaviour, the assumed rigid particles are allowed to have small overlapping contact, and thus contact forces are developed as a result of particular stiffness and/or damping characteristics. The technique establishes a discretized time stepping numerical routine, in which granule velocities and positions are obtained through numerical integration of the computed accelerations. Using the principle of *causality*, it follows that during an appropriately small time step, disturbances cannot propagate from any disk further than its immediate neighbours. Under these conditions, the method becomes explicit, and therefore at any time increment the resultant forces (and thus the accelerations) on any particle are determined solely by its interactions with its contacting neighbours. For applications to wave propagation, the movements of the individual disks are a result of the propagation through the medium of disturbances originating at particular input loading points. Consequently, the wave speed and amplitude attenuation (intergranular contact force) will be functions of the physical properties of the discrete medium, i.e. the microstructure or fabric.

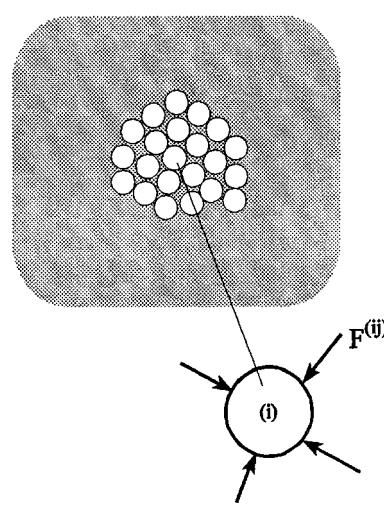

Figure 3. Discrete element modelling

The general concept of the method may be explained by considering a general two-dimensional particulate assembly as shown in Figure 3. Isolating attention to the ith particle and applying Newton's laws yields

$$\begin{aligned} \sum_{j=1}^{N} F^{ij} + F^{i} &= m_i \ddot{x}_i \\ \sum_{j=1}^{N} M^{ij} + M^{i} &= I_i \ddot{\theta}_i \end{aligned} \tag{1}$$

where F^{ij} are the j contact forces on the ith particle, F^i represents any non-contacting forces on particle i, M^{ij} are the moments (about the particle's mass centre) resulting from contact forces F^{ij}, M^i is the resultant moment from any non-contacting forces, m_i is the particle mass, and I_i is the mass moment of inertia. With given contact and non-contact forces, the linear and angular accelerations of the ith particle can thus be determined from this system of equations. With the accelerations known, the velocities and displacements may be obtained through numerical integration using simple finite differencing schemes.

It is obvious that the contact response between neighbouring particles plays a very important role in the use of this numerical method to simulate wave propagation through granular materials. Past research, Sadd *et al.*[28] has investigated the use of several contact laws within the discrete element modelling scheme. Establishing a local normal and tangential co-ordinate system at each contact between adjacent particles, a contact law can be constructed relating interparticle force to the overlapping deformation and deformation rate. In general such a contact law between adjacent particles could be written as

$$\begin{aligned} F_n^{ij} &= F_n^{ij}(\delta_n, v_n, \delta_t, v_t) \\ F_t^{ij} &= F_t^{ij}(\delta_n, v_n, \delta_t, v_t) \end{aligned} \tag{2}$$

where δ_n and δ_t are the relative normal and tangential displacements between particles i and j, and v_n and v_t are the relative normal and tangential velocities. Contact relations (2) may also be *history dependent*, and a Coulomb-type friction law is commonly incorporated to place limits on the tangential response. Specific forms of such contact relations have included[28] linear, non-linear, and non-linear hysteretic laws. Results have indicated that the non-linear hysteretic deformation law provided simulation results which compared favourably with experimental data,[28] and this particular law has been chosen for use in the current study.

BRANCH VECTOR FABRIC

One popular fabric measure used for the static response of granular materials has been the *branch vector*. This measure is defined as the vector drawn between the mass centres of contacting particles, see Figure 1. For the circular particles under study, dynamic loads are transmitted primarily through contact points which lie along branch vectors, and thus this fabric measure appears to be appropriate for wave propagation problems. Thus it seems reasonable to assume that branch vector distributions could be related to the wave propagational behaviours in such media.

To investigate such relationships, several large random particulate media assemblies were numerically generated. All assemblies contained 25 mm diameter particles of equal size. Generation schemes used various algorithms[29] to construct model assemblies with different microstructures as reflected in the distributions of branch vectors. These distributions can be classified as *strongly*, *moderately and weakly anisotropic* model systems. Six such assemblies are shown in Figure 4; where assembly S-1 was generated by a strongly anisotropic generator, assemblies

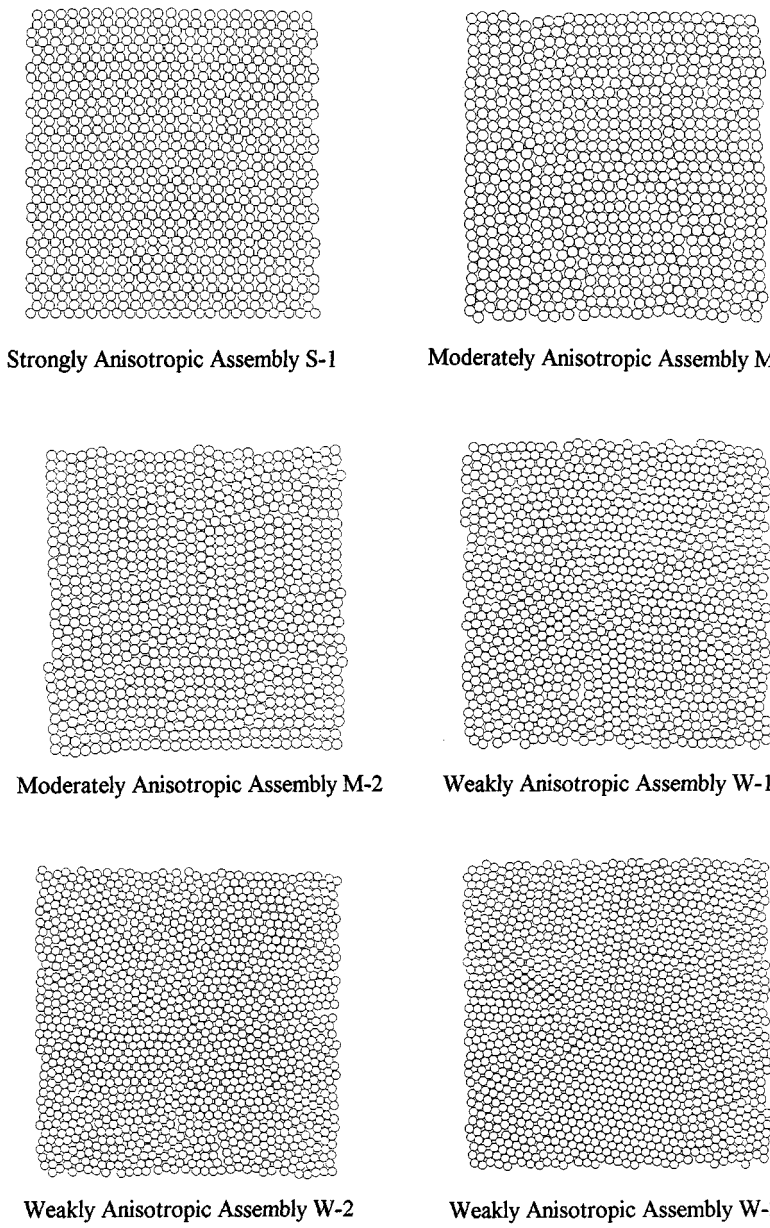

Figure 4. Six model granular material systems

M-1 and M-2 were constructed by a moderately anisotropic generator, and a weakly anisotropic scheme was used to construct assemblies W-1, W-2 and W-3. Table I lists additional parameters for each of these assemblies including the total numbers of particles, the void ratio (volume of void/volume of particle) and the average co-ordination number (average number of contacts per particle). Assembly S-1 has the highest void ratio of 0·43 and lowest coordination

Table I. Summary of various fabric measures and wave transmissions for six model assemblies

Assembly	No. of particles	Void ratio	Coor. no	R_F	R_b	R_p	R_v
S-1	822	0·43	2·87	200·7	2·06	No path$_x$	85·18
M-1	778	0·28	3·43	33·3	1·19	5·88	2·44
M-2	854	0·28	3·41	100·0	1·19	2·08	2·58
W-1	1042	0·25	4·17	1·7	1·01	0·95	1·12
W-2	1296	0·25	4·04	0·9	0·99	1·00	1·05
W-3	1338	0·22	4·30	1·2	1·01	1·16	1·00

number of 2·87, while W-3 has the lowest void ratio of 0·22 and the highest co-ordinate number of 4·30.

Although it would be desirable to develop general relationships between fabric vectors/tensors and wave propagational variables, the current state of knowledge requires a simpler, pragmatic approach. Thus in order to investigate the relationship between branch vector fabric and wave propagational characteristics, all unit branch vectors were calculated for each assembly. Polar distributions of these branch vectors were then determined and are shown in Figure 5. In order to quantify such distributions, a *branch vector ratio*

$$R_b = \sum |b_y| / \sum |b_x| \tag{3}$$

was calculated, where b_x and b_y are horizontal and vertical components of the unit branch vectors, and the summations go over all defined branch vectors in a given model assembly. Values of the ratio R_b for the six assemblies are listed in Table I. For assembly S-1, all branch vectors are concentrated in the region approximately defined by $\pm 30^\circ$ from the vertical direction. No branch vector is found along the horizontal direction, and R_b is 2·06 for this assembly. The branch vector distributions for assemblies M-1 and M-2 primarily occur in vertical and horizontal directions with preference in vertical direction, and both assemblies have the same R_b ratio of 1·19. For the weakly anisotropic assemblies W-1, W-2 and W-3, no highly preferred branch vector directions were found, and the branch ratios for these cases were all close to unity.

Each of the six constructed assemblies were subjected to dynamic loadings to create a wave propagation situation, and this behaviour was modelled using our discrete element wave propagation code. The simulations involved the comparison of the propagation of plane type waves moving along horizontal (x-direction) and vertical (y-direction) paths in the generated assemblies. To generate the plane vertical wave, all particles along the bottom of the assembly were simultaneously loaded in the vertical direction with a transient input loading of triangular time history. The input pulse had a peak value of 1 kN and a period of 60 μs. From a continuum point of view, this type of loading will input primarily a planar P or dilatational wave. Of course, as the combined dynamic signal moves through the granular medium, some small tangential interparticle contact forces will develop, and thus at the microlevel, there will be some partitioning of the signal into the *shearing mode*. We would not however, classify this mode as a shear wave component. The generated input for the horizontal wave was created in a similar fashion.

To calculate the transmitted or output wave pulse, an imaginary horizontal or vertical line was drawn near the boundary opposite to where the input loadings were applied. If a branch vector of a pair of particles in contact or potential contact is intercepted by this imaginary line, the normal contact load component perpendicular to the imaginary line, i.e. either F_x or F_y, was recorded. In this fashion, the contribution of the individual particle contacts could be determined, and these recorded loads were then summed and normalized with respect to the sum of the peak values

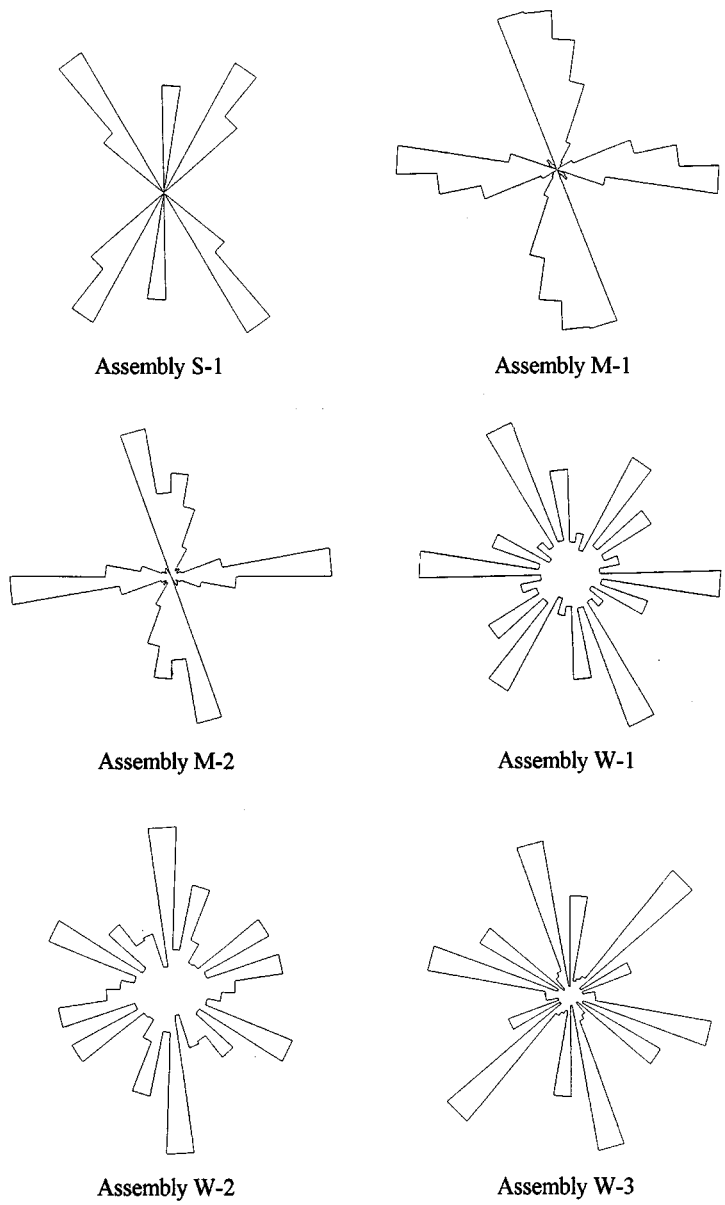

Figure 5. Branch vector distribution plots of model assemblies

of the input loadings. These normalized contact loads or *load transmission ratios* for horizontal and vertical waves are thus given by

$$\bar{F}_x(t) = \frac{\sum F_x(t)}{\sum F_{\text{peak input}}}$$
$$\bar{F}_y(t) = \frac{\sum F_y(t)}{\sum F_{\text{peak input}}} \tag{4}$$

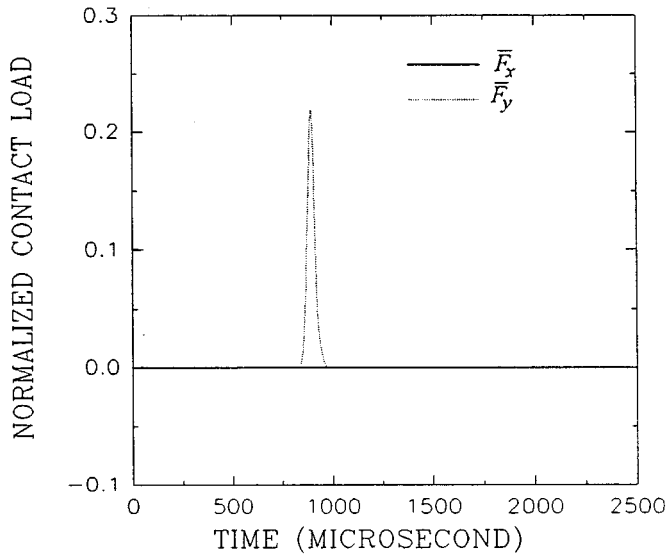

Figure 6. Wave transmission results for assembly S-1

where the summation in the numerator is over the number of branch vectors intercepted by the imaginary line, while the summation in the denominator is over the number of input loadings. In order to compare these horizontal and vertical transmission ratios, the ratio of their peak values may be used, i.e.

$$R_F = \{\bar{F}_y(t)\}_{\text{peak}} / \{\bar{F}_x(t)\}_{\text{peak}} \tag{5}$$

This ratio is given in Table I for each of the six assemblies under study.

Figure 6 shows the transmission results of a discrete element wave propagation simulation for the media model S-1, and it is quite apparent that the vertical, y-component of load transmission is predominant for this assembly. Although it is not discernable from the figure, the wave speed as determined by the arrival time of these averaged transmission profiles is different for the two propagational directions, with a vertical wave speed approximately three times that of the horizontal motion. These results correlate with the branch vector distribution plot shown in Figure 5(a), thus indicating that the branch vector is related to the transmission of waves in particulate materials. Similar results occur for the moderately anisotropic assemblies M-1 and M-2; however, for these cases the fabric ratio R_b fails to correlate completely with the numerical model simulation results. For example, both the peak transmission ratios R_F and the wave speeds indicate that model assembly M-2 is more anisotropic than assembly M-1, but unfortunately this does not correlate with their branch fabric ratios as given in Table I. The wave transmission results for the weakly anisotropic assembly W-2 are shown in Figure 7. Table I indicates that the R_F ratio for this case is much smaller than for the strongly and moderately anisotropic assemblies, and this correlates reasonably well with branch vector fabric.

PATH FABRIC

As mentioned previously, when waves propagate through granular media, the local or micro-dynamic loads are transferred through specific chains of particles linked through contact.

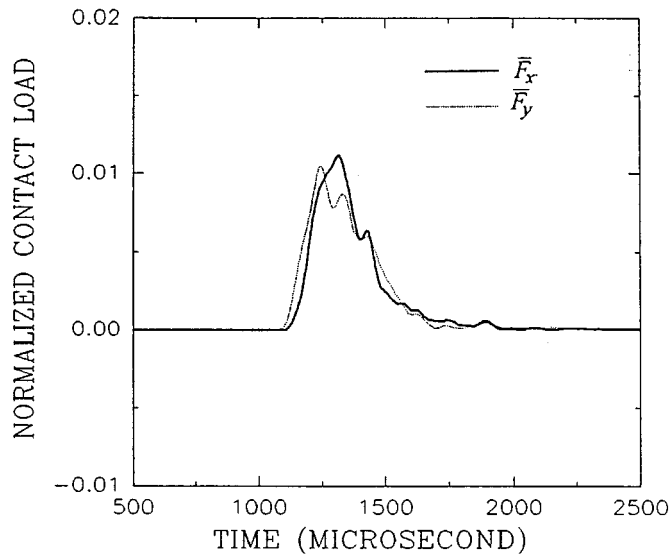

Figure 7. Wave transmission results for assembly W-2

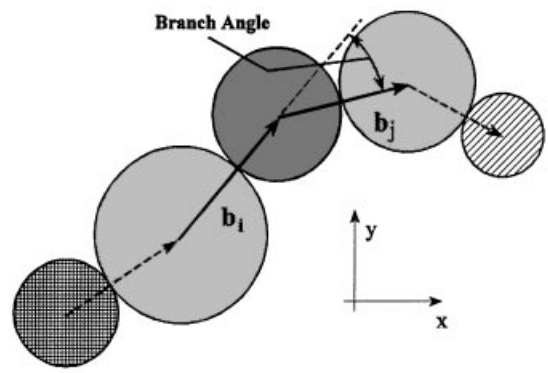

Figure 8. Schematic of path fabric concept

Between these special chains, particles may carry little or no load. It would be expected that such load carrying paths which are relatively straight would act as a better propagator of waves than would a highly irregular path. Thus it appears that the local microstructure of load carrying paths within a particulate medium would also be an appropriate fabric measure to correlate with wave propagation.

In order to quantify the path fabric concept, a path is defined as a set of continuous branch vectors of particles in contact as shown in Figure 8. It has been observed experimentally by Shukla and Damania[30] that for dry cohesionless materials, dynamic load can be transferred along a path only when every pair of neighbouring branch vectors $\mathbf{b}_i$ and $\mathbf{b}_j$ in the path satisfy the relationship

$$\mathbf{b}_i \cdot \mathbf{b}_j > 0 \tag{6}$$

which means that the *branch angle* defined in Figure 8 is less than 90°. Therefore, a *transferable* or *propagator load path* can be defined as a path in which the dot product of all pairs of neighbouring branch vectors is positive.

One method of constructing a path fabric measure, based on the straightness of the path, would be to sum the dot products of all adjacent unit branch vectors in a given propagator path. For example, a path fabric measure between two arbitrary particles could be expressed as

$$F_p = \sum \frac{1}{\sum \frac{1}{\mathbf{b}_i \cdot \mathbf{b}_j}} \tag{7}$$

where the inner summation is over all connecting particles on a given path, while the outer summation is over all possible paths. For the special case of a single straight chain of particles, there exists only one path between any two particles, and equation (7) gives $F_p = 1/(N-1)$, where N is the total number of particles in the path. This would constitute a minimum value of F_p among all assemblies of single particulate chains.

Another method to construct a path fabric measure is to use x and y branch vector components by defining the following quantities between two arbitrary particles

$$\begin{aligned} \bar{P}_x &= \sum\sum |b_x| / \sum\sum 1 \\ \bar{P}_y &= \sum\sum |b_y| / \sum\sum 1 \end{aligned} \tag{8}$$

where outer summations are over all possible paths between the two arbitrary particles, and inner summations are over individual paths. For granular media simulated by circular particles of the same size, the values of $\bar{P}_x$ and $\bar{P}_y$ will not be larger than the particle diameter, and will equal to the diameter only when the path is a straight chain along the x or y direction.

In order to do the necessary calculations specified by equation (7) or equation (8), considerable computational effort is required for the six assemblies under study. All propagator paths must be determined in these assemblies between input and output particles for both horizontal and vertical wave propagation simulations. Such calculations for assemblies with 10^3 particles typically yield 10^7–10^8 total possible paths. In order to reduce the size of this computational problem, the model assemblies are divided into subregions, and paths outside prescribed boundaries will be discarded.

Figure 9 illustrates such a scheme for the calculation of vertical propagation paths. A particular vertical propagator path is shown between a pair of arbitrary input and output particles. Equation (8) for this vertical path can be written as

$$\begin{aligned} \bar{P}_x &= \frac{\sum\sum P_x}{\sum\sum 1} = \frac{N_{\text{path}}}{\sum\limits_{\text{path}} N_{\text{particle}}} P_x \\ \bar{P}_y &= \frac{\sum\sum P_y}{\sum\sum 1} = \frac{N_{\text{path}}}{\sum\limits_{\text{path}} N_{\text{particle}}} P_y \end{aligned} \tag{9}$$

where P_x and P_y are the x and y components of the vector from the input particle to the output particle, N_{path} is the total number of paths between the input and output particles, and N_{particle} is the total number of particles along the given path. The determination of the number of paths and the number of particles on a given path may be carried out through calculations in subregions,[29] e.g. regions I–III shown in Figure 9. It should be pointed out that a particular vertical path under consideration will be discarded if it extends beyond a vertical zone of fixed width centred at the

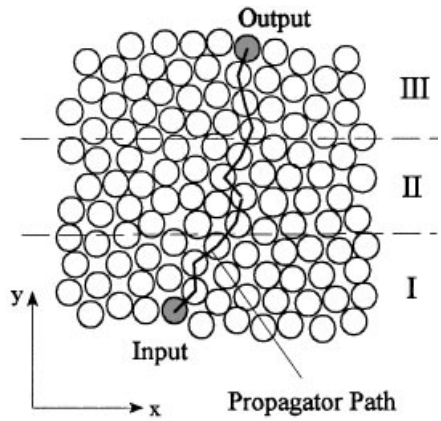

Figure 9. Vertical propagator path

initiating input particle within a subregion. This is reasonable since a highly tortuous path will transmit negligible load, and by discarding these paths a reduction of computational effort will result. The vertical path fabric measure for the whole assembly can then be obtained by summing the values given by equation (9), for all the paths between all input and output boundary particles.

Using equation (9), the vertical and horizontal path fabrics of each of the six model assemblies have been computed. The ratios of the summations of vertical fabric to the summations of horizontal fabric

$$R_p = \sum \bar{P}_y / \sum \bar{P}_x \tag{10}$$

are given in Table I. For the strongly anisotropic assembly S-1, there is no contiguous path along the horizontal direction and this gives a ratio of infinity, which correlates with the discrete element results which show that the horizontal wave is almost blocked. The R_p ratio has values of 5·88 and 2·08 for the two moderately anisotropic assemblies M-1 and M-2. Thus, there are more paths along the vertical direction rather than the horizontal direction, and waves prefer to propagate along the vertical direction in these assemblies as predicted by discrete element analysis. However, as with the branch vector case, the path fabric also fails to correlate with the stronger wave propagation anisotropy of assembly M-2 with respect to assembly M-1. The reason for this lack of correlation may be due to gap closing during the passage of the wave motion, and such phenomena can change the path fabric. Taking assembly M-2 as an example, during the process of vertical wave propagation, it appeared from our discrete element modelling that more than 40 new contacts had been created. The R_p ratios of the weakly anisotropic assemblies W-1, W-2, and W-3 are 0·95, 1·00, and 1·16, respectively, which indicates that these assemblies are indeed weakly anisotropic. These ratios provide a reasonable correlation between path fabric and wave behaviours for the W-assemblies.

VOID POLYGON VECTOR FABRIC

The previous two sections proposed fabric measures associated with the particles of granular systems. However, in addition to the solid particle phase, a granular material also consists of a void phase, and thus it would seem reasonable that a fabric measure based on voids could be

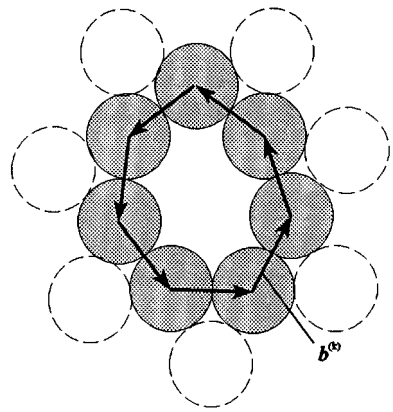

Figure 10. Void fabric schematic

useful to correlate with wave propagation. This concept of using voids to characterize fabric was first proposed by Konishi and Naruse[18] for the static response of particulate materials.

To describe a void with N curved segments, a polygon is used as shown in Figure 10. The polygon consists of the branch vectors linking the particles around a void, and thus a *void polygon* is represented by this special group of branch vectors. Assuming that a void surrounded by N particles has N branch vectors $\mathbf{b}^{(1)}, \mathbf{b}^{(2)}, \ldots,$ and $\mathbf{b}^{(N)}$, a *local void tensor* can be defined as

$$p_{ij} = \sum_{k=1}^{N} b_i^{(k)} b_j^{(k)} \tag{11}$$

where $b_i^{(k)}$ are the components of $\mathbf{b}^{(k)}$. The principal values of this void tensor are given by

$$p_1, p_2 = \frac{1}{2} \sum_{k=1}^{N} b_k^2 \pm \sqrt{\left[\left(\sum_{k=1}^{N} b_k^2 \cos 2\theta_k \right)^2 + \left(\sum_{k=1}^{N} b_k^2 \sin 2\theta_k \right)^2 \right]} \tag{12}$$

and the major principal direction is calculated as

$$\theta_p = \frac{1}{2} \arctan \left[\left(\sum_{k=1}^{N} b_k^2 \sin 2\theta_k \right) \Big/ \left(\sum_{k=1}^{N} b_k^2 \cos 2\theta_k \right) \right] \tag{13}$$

Now a void can be described by the set $\{p_1, p_2, \theta_p\}$ in the following manner: $H = p_1 - p_2$ is related to the void anisotropy, $S = p_1 p_2$ represents the void area, and θ_p specifies the void orientation or direction. Konishi and Naruse[18] proposed a fabric measure based on a *local void vector* $\mathbf{p}$ with magnitude H and direction specified by θ_p. A modification of this definition is used in this study, whereby the void vector $\mathbf{p}$ is defined as a vector whose magnitude is HS with direction coinciding with the major principal axis. The reason for including S in the void vector definition is based on the premise that void size (area) will play a role in the dynamic response of granular materials, and thus it should appear explicitly in a proposed fabric measure. It should be pointed out that for the case of isotropic voids, $H = 0$, thus implying a zero void vector. However, this would be an unlikely situation for granular media generated through the random procedures used in this study.

Using this scheme of local void vectors, a polar rose diagram can be constructed similar to the branch vector distributions in Figure 4, and these plots are shown in Figure 11 for the six model

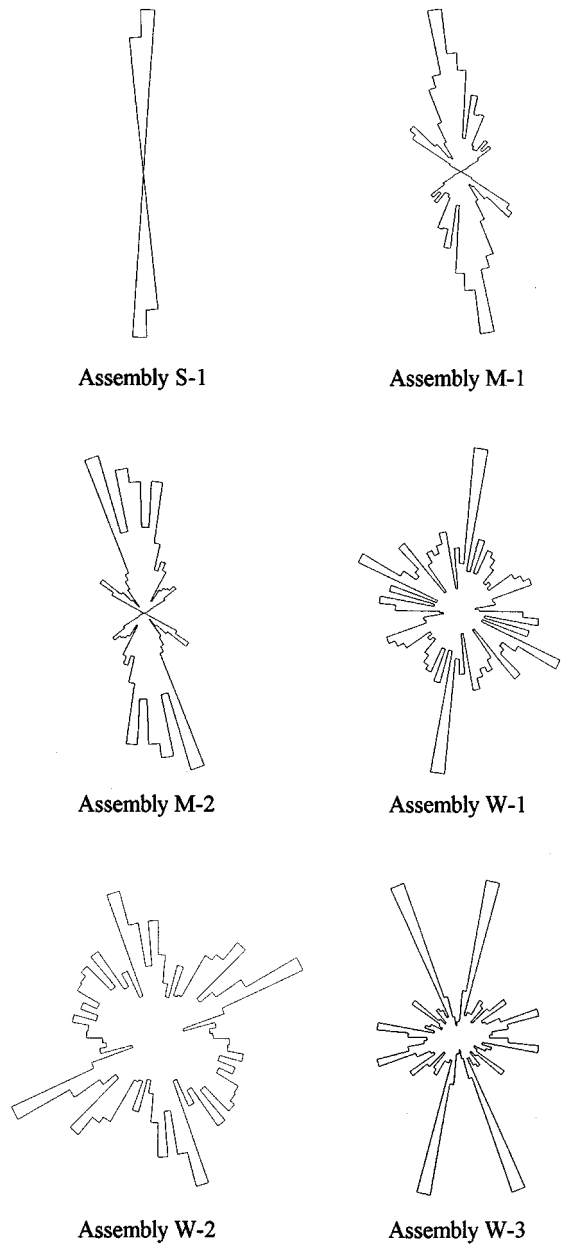

Figure 11. Void vector distribution plots of model assemblies

assemblies under study. An examination of these plots along with a comparison of the corresponding branch vector diagrams reveals that void vector distributions appear to have some advantages in correlating wave propagation with the material microstructure. In the void vector distribution diagram for assembly S-1, all void vectors lie in the vertical direction to block horizontal wave paths, while the corresponding branch vector diagram fails to demonstrate this.

For assemblies M-1 and M-2, the void vector diagrams show an overwhelming majority of void vectors lying in the vertical direction. This agrees with the numerical wave motion simulations, while the corresponding branch vector diagrams only show slightly more branch vectors in vertical direction than in the horizontal. The void vector diagrams for the W-assemblies also indicate preferred wave propagation directions, which was not apparent in the branch vector diagrams.

A *void vector ratio* defined as all void vector components in the vertical direction over all components in the horizontal, i.e.

$$R_v = \sum p_y / \sum p_x \tag{14}$$

can thus be used to measure the anisotropy of a medium with respect to voids. The values of this ratio R_v, for the six assemblies are given in Table I. This ratio generally increases with the degree of assembly anisotropy except for assemblies W-2 and W-3, and it has a maximum value for assembly S-1, thus indicating the strongly anisotropic properties of this model medium. For moderately anisotropic assemblies M-1 and M-2, the ratio decreases and successfully predicts a stronger anisotropy for assembly M-2 with respect to M-1. The values of R_v for the weakly anisotropic assemblies W-1, W-2 and W-3 are all close to unity. The void fabric ratio correctly indicates that the degrees of anisotropy in W-2 and W-3 are smaller than in W-1, but as with the other fabric measures it fails to identify W-2 as having the smallest degree of wave attenuation anisotropy among the W-assemblies. These differences among the W-assemblies are however, relatively small.

CONCLUSIONS

Results of several discrete element simulations of wave propagation through model granular materials have been presented. The model materials included six numerically generated assemblies of circular particles with prescribed initial fabric anisotropy varying from strongly to weakly anisotropic. Plane type wave propagations were simulated in horizontal and vertical directions through each assembly by applying dynamic loadings to appropriate boundary particles. Wave propagation behaviour such as wave speed and amplitude attenuation were determined from the discrete element model using specific non-linear hysteretic interparticle contact laws developed in previous research.

In order to establish relationships between these simulated propagational characteristics and granular microstructure, specific fabric measures were employed. Based on observed experimental information and on previous studies, three particular fabric descriptors were chosen including branch vectors, path microstructures, and void characteristics. The spatial distributions of these fabric measures were determined for each of the six model assemblies under study. These distributions were then averaged over each assembly with respect to horizontal and vertical directions, and comparisons were made with the discrete element wave propagational results. It should be noted that the wave propagation-fabric relationships are thus limited to the simulations in the horizontal and vertical coordinate system. Planar wave propagation in other directions would be difficult to simulate in these assembly models.

Findings of the study indicated that each of the three fabric descriptors provided a reasonable degree of correlation with the wave motion results, and that the void vector fabric measure appeared to provide the best correlation for the six model materials. However, even though each model material system was randomly generated and contained hundreds of particles, it is not possible to argue the point in general, that void fabric will be a better microstructural measure than branch vector or load/propagator path fabric schemes. Clearly additional research is needed

to further narrow the wide choices of appropriate fabric measures to predict the dynamic response of granular materials.

It should be pointed out that in addition to microstructure or fabric, wave propagation in particulate media is also frequency or wavelength dependent. This type of medium acts as a non-linear wave guide, and local microstructure and contact non-linearity will produce dispersive, frequency-dependent propagational behaviours. This aspect has been investigated by us[31] in some detail for one-dimensional material models. One particular aspect which was observed both experimentally and numerically was that signals of sufficiently long wavelength can excite resonant subunits of the medium. For this behaviour, a smooth input signal will undergo separation into a series of short oscillatory wave forms, and this repartitioning of energy effects the local attenuation response. The 60 μs input pulse used in this study was sufficiently short enough so as not to produce this effect. Although it appears from the output signals shown in Figures 6 and 7 that wave form spreading has occurred, in reality this results from the fact that *averaged* output wave signals are being plotted. The averaging process sums individual contributions from several contacts along the output side of the assembly model, and because of small time shifts of each of the various signals, the time signature of the summed signal is broader (200–500 μs) than the individual signals (60 μs). The current study did not investigate frequency effects nor vary the input loading duration.

A longer-term goal of this type of research would be to construct general relationships to connect wave propagation variables with averaged microfabric. For example, if we define volume-averaged, second-order fabric tensors based on branch vectors $\bar{F}_{ij}^{(b)}$, path vectors $\bar{F}_{ij}^{(p)}$, and void vectors $\bar{F}_{ij}^{(v)}$, then it would be desirable to develop a general wave transmission law of the form

$$\mathrm{TR} = f(\bar{F}_{ij}^{(b)}, \bar{F}_{ij}^{(p)}, \bar{F}_{ij}^{(v)}) \tag{15}$$

where TR would represent the amplitude transmission ratio of output to input. This effort is currently underway. Clearly experimental determination of particulate media microstructural fabric is needed to be able to use such theoretical relationships. Such efforts to determine microstructure or fabric of actual granular materials have been conducted, see for example Gill[32] or Hryciw and Raschke.[33]

ACKNOWLEDGEMENTS

The authors would like to express their appreciation to the Air Force Office Scientific Research — Particulate Mechanics Program, who under Contract No.s F49620-89-C-0091 and F49620-93-1-0209 supported the research herein described.

REFERENCES

1. M. Oda, S. Nemat-Nasser and M. M. Mehrabadi, 'A statistical study of fabric in a random assembly of spherical granules', *Int. j. numer. anal. methods geomech.*, **6,** 77–94 (1982).
2. C. Y. Zhu, A. Shukla and M. H. Sadd, 'Prediction of dynamic contact loads in granular assemblies', *J. Appl. Mech.*, **58,** 341–346 (1991).
3. A. Shukla, C. Y. Zhu and M. H. Sadd, 'Angular dependence of dynamic load due to explosive loading in two dimensional granular aggregate', *J. Strain Anal.*, **23,** 121–127 (1988).
4. J. Duffy and R. D. Mindlin, 'Stress–strain relations and vibrations of a granular medium', *J. Appl. Mech.*, **24,** 585–593 (1957).
5. H. Deresiewicz, 'Stress–strain relations for a simple model of a granular medium', *J. Appl. Mech.*, **25,** 402–406 (1958).
6. J. Duffy, 'A differential stress–strain relation for the hexagonal close-packed array of elastic spheres', *J. Appl. Mech.*, **26,** 88–94 (1959).
7. B. O. Hardin and G. E. Blandford, 'Elasticity of particulate materials', *J. Geotech. Eng.*, **115,** 788–805 (1989).

8. P. J. Digby, 'The effective elastic moduli of porous granular rocks', *J. Appl. Mech.*, **48,** 803–808 (1981).
9. C. Thornton and D. J. Barnes, 'Computer simulated deformation of compact granular assemblies', *Acta Mech.*, **64,** 45–61 (1986).
10. E. Petrakis and R. Dobry, 'A two-dimensional numerical micromechanical model for a granular cohesionless materials at small strains', *Proc. Am. Phys. Soc.*, New Orleans, LA, 1988.
11. E. Petrakis, R. Dobry and T. Ng, 'Small strain response of random arrays of elastic spheres using a nonlinear distinct element procedure', *Report CE-88-02, Resselaer Polytechnic Institute*, Troy, NY, 1988.
12. Y. Kishino, 'Disc model analysis of granular media', in M. Satake and J. T. Jenkins, (eds) *Micromechanics of Granular Materials.* Elsevier, Amsterdam, 1988.
13. C. S. Chang and L. Ma, 'Modeling of discrete granulates as micropolar continua', *J. Eng. Mech.*, **116,** 2703–2721 (1990).
14. O. Walton, 'The effective elastic moduli of a random packing of spheres', *J. Mech. Phys. Solids*, **35,** 213–226 (1987).
15. M. Oda, S. Nemat-Nasser and M. M. Mehrabadi, 'A statistical study of fabric in a random assembly of spherical granules', *Int. j. numer. anal. methods geomech.*, **6,** 77–94 (1982).
16. S. Nemat-Nasser and M. M. Mehrabadi, 'Stress and fabric in granular masses', in J. T. Jenkins and M. Satake (eds) *Mechanics of Granular Materials*: *New Models and Constitutive Relations*, Elsevier, Amsterdam, 1983.
17. R. J. Bathurst and L. Rothenburg, 'Micromechanical aspects of isotropic granular assemblies with linear contact interactions', *J. Appl. Mech.*, **55,** 17–23 (1988).
18. J. Konshi and F. Naruse, 'A note on fabric in terms of voids', in M. Satake and J. T. Jenkins (eds) *Micromechanics of Granular Materials*, Elsevier, Amsterdam, 1988.
19. M. Satake, 'A discrete-mechanical approach to granular materials', *Int. J. Eng. Sci.*, **30,** 1525–1533 (1992).
20. T. Bourbié, O. Coussy and B. Zinszner, *Acoustics of Porous Media*, Gulf Publishing, Houston, 1987.
21. P. A. Cundall and O. D. L. Strack, 'A discrete numerical model for granular assemblies', *Geotechnique*, **29,** 47–65 (1979).
22. C. Thorton and C. W. Randall, 'Appications of theoretical contact mechanics to solid particle system simulation', in M. Satake and J. T. Jenkins (eds) *Micromechanics of Granular Media*, Elsevier, Amsterdam, 1988.
23. J. Ting, B. T. Corkum, C. Kauffman and C. Greco, 'Discrete numerical model for soil mechanics', *J. Geotech. Eng.*, **115,** 379–398 (1989).
24. J. R. Williams, 'Contact analysis of large numbers of interacting bodies using modal methods for microscopic failure analysis', *Int. J. Comp. Aided Methods in Eng.*, **5** (1988).
25. O. R. Walton, D. M. Maddix, T. R. Butkovich and F. E. Heuze, 'Redirection of dynamic compressive waves in materials with nearly orthogonal and random joint sets', *Proc. ASME Appl. Mech. Conf. on Recent Adv. in Mech. of Structured Continua*, Columbus, OH, 1991.
26. T. T. Ng and R. Dobry, 'A non-linear numerical model for soil mechanics', *Int. J. Non-linear Mech.*, **16,** 247–263 (1992).
27. L. Rothenburg and R. J. Bathurst, 'Influence of particle eccentricity on micromechanical behavior of granular materials', *Mech. Mat.*, **16,** 141–152 (1993).
28. M. H. Sadd, Q. M. Tai and A. Shukla, 'Contact law effects on wave propagation in particulate materials using distinct element modeling', *Int. J. Non-linear Mech.*, **28,** 251–265 (1993).
29. Q. M. Tai, *Ph.D. Thesis*, University of Rhode Island, 1993.
30. A. Shukla and C. Damania, 'Experimental investigation of wave velocity and dynamic contact stresses in an assembly for disks', *Exp. Mech.*, **27,** 268–281 (1987).
31. A. Shukla, M. H. Sadd, Y. Xu and Q. M. Tai, 'Influence of loading pulse duration on dynamic load transfer in a simulated granular medium', *J. Mech. Phys. Solids*, **41,** 1795–1808 (1993).
32. J. J. Gill, 'The microstructural response of granular soil under uniaxial strain', *Report No. PL-TR-92-1064*, Phillips Laboratory, Kirtland AFB, NM, 1993.
33. R. D. Hryciw and S. C. Raschke, 'Soil characterization and experimental micromechanics through computer vision and digital image processing', *AFOSR Particulate Mechanics Contractor's Meeting*, Tyndall AFB, FL, September 1995.

